



Random laser based method for direct measurement of scattering properties

FEDERICO TOMMASI,* EMILIO IGNESTI, LORENZO FINI, FABRIZIO MARTELLI, AND STEFANO CAVALIERI

Dipartimento di Fisica e Astronomia, Università di Firenze, via G. Sansone 1, I-50019 Sesto Fiorentino, Italy

*federico.tommasi@unifi.it

Abstract: Optical sensing is a very important method for investigating different kinds of samples. Recently, we proposed a new kind of optical sensor based on random lasing [Sci. Rep. **6**, 35225 (2016)], that couples the advantages of stimulated emission in detecting small variations on scattering properties of a sensed material, to the needs of no alteration of the sample under investigation. Here, we present a method to achieve a quantitative measurement of the scattering properties of a material. The results on samples of calibrated microspheres show a dependence of the peak intensity of the emission spectrum on the transport mean free path of the light within the sample, whatever the dimension (down to ≈ 100 nm of particle diameter) and the concentration of scatterers dispersed in the sensed material. A direct and fast measurement of the scattering properties is obtained by calibration with a well-known and inexpensive reference medium.

© 2018 Optical Society of America under the terms of the [OSA Open Access Publishing Agreement](#)

1. Introduction

The development of optical sensors has been extensively carried on during the last two decades in different fields, like medical diagnostic and material characterization [1–3]. The theoretical and experimental efforts in developing optical sensors have been stimulated by the advantages offered by these devices. In particular, an optics-based sensing strategy can prove to be less invasive respect to other methods, making that kind of detection an established tool to study biological samples, in particular for *in-vivo* applications.

In a scenario where the great majority of these strategies developed until now are based on “passive” optical phenomena, i.e. the light emitted by a source undergoes attenuation by propagation through the sensed medium, we recently proposed a new kind of “active” sensor [4]. With the term “active” we mean a method that involves the amplification and modification of the original signal by the interaction between the sensor and the sensed sample. Here we present a work where such active sensor has been used to provide a method for direct measurement of scattering properties.

Two important optical properties of a material that can be investigated by optical sensing are scattering and absorption. The scattering, in particular, can give valuable information about the granular nature and the microstructure of the sample material. The optical properties of a material are described by three macroscopic parameters: the absorption coefficient μ_a , the scattering coefficient μ_s and the reduced scattering coefficient μ'_s . μ_s and μ'_s are the reciprocal of the scattering mean free path ℓ_s and the transport mean free path ℓ_t respectively. In statistical meaning, the former is the average distance between two successive scattering events, while the latter is the average traveling distance of the photons after which the radiation can be considered as isotropically diffused. The two coefficients are bounded each other by the relation $\mu'_s = \mu_s(1 - g)$, where g is the asymmetry factor of the scattering function [5].

Experimentally, in particular for highly scattering media, the measurement of these properties is typically a non-trivial procedure that has been carried out by different methods during the last decades. The techniques can be roughly classified in two main classes [6]:

- a) direct measurements of the optical properties, where the measured quantities are directly related to the optical properties
- b) indirect measurements, where an interaction model and an inversion complex procedure are needed to reconstruct the values of the optical properties

Direct measurements of the optical properties are difficult to be done and only few examples of these methods can be found. For instance, in the first class can be classified the methodology for measuring the extinction coefficient where a thin sample of medium of known thickness is used [7]. This technique, by using the Lambert-Beer law, allows to determine the extinction coefficient, $\mu_t = \mu_a + \mu_s$, of the medium. For media with negligible absorption, μ_s can thus be obtained, and vice-versa when the scattering is negligible μ_a can be determined. In the techniques of the second class the optical properties are obtained by making use of complex models for light propagation and of non-linear regression procedures [8]. The measured quantities are usually the diffuse reflectance, or the transmittance, or the fluence rate [9, 10]. Mathematical models are used to reconstruct the absorption and the reduced scattering coefficients of the medium from the measured quantity by inversion procedures (inverse problem). Depending on the kind of excitation source, the different techniques are also usually classified in continuous wave (CW) domain, time domain (TD) and frequency domain (FD) approaches [8–16]. The present contribution is addressed to characterize the scattering properties of a turbid medium. Although these methods nowadays show a high level of precision and reliability, the introduction of easy to use new methods is very interesting for practical applications. Hence, besides the passive optical methods cited above, different experimental strategies have been explored to exploit the stimulated emission mechanism in the analysis of biological systems [17, 18].

The random laser is another example of a phenomenon based on stimulated emission [19]. Such an optical source is a type of optical emission that arises from the combined effect of scattering and stimulated emission of photons that propagate within a disordered medium, where a pumping system has established a population inversion. The output emission of this optical source shows a halfway behavior between a natural incoherent source and a laser; if the gain along random paths of light inside the disordered active medium becomes strong enough to overcome the losses, a spectral narrowing, due to the stimulated emission prevails the spontaneous one without the need of the optical cavity, and the main effects over the output are a narrowing and a shift of the emission spectrum. The properties of this kind of optical source have been extensively investigated since the 90's [20]. The striking point is that the random laser emission is basically due to the scattering properties of the medium, making the random laser a natural candidate for studying scattering media [21, 22]. Very recently, sensors based on random laser emission have been proposed to measure the pH of a liquid [23] and to detect ultrasounds in solid materials [24]. Random laser emission has been obtained in several kinds of materials, such as powder of laser crystal [25–27], nanoparticles dispersed in dye alcoholic solution, [28–32] and in general whatever material able to scatter and amplify light. In particular, biological tissues are an important category of scattering media at visible and NIR wavelengths (in particular from 600 nm to 900 nm). Some promising experimental works have been reported on biological *ex-vivo* samples: chicken tissue and pig fat [33], rat muscle [34] and chicken breast tissue [35], bovine bone [36], wing of cicada covered with a layer of a dye doped polymer film [37] and butterfly embedded with ZnO nanoparticles [38]. Moreover, a clear difference in random laser spectra, from a dye infiltrated *ex-vivo* human tissue, between a malignant tissue compared to the healthy one has been reported [39, 40], as well as the possibility to explore new forms of opto-chemical therapies for cancer [41]. However, despite its very interesting peculiar features and its longstanding studies, applications based on random laser are still confined to the research level. One reason for that involves the need to inject external toxic gain material inside the sensed media and to irradiate the sample with the pump beam, making impossible the perspectives of

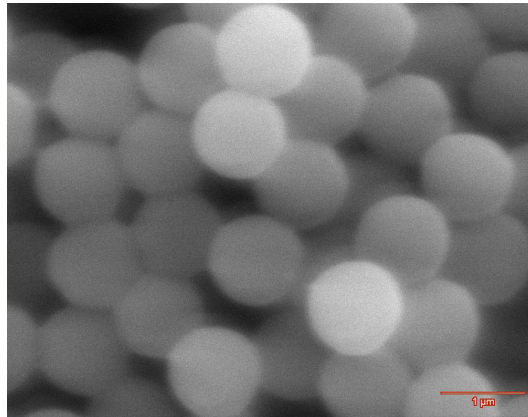


Fig. 1. A latex spheres sample provided by Magsphere Inc. at electron microscope.

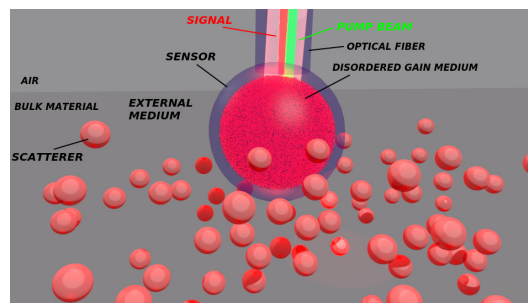


Fig. 2. Scheme of the sensor structure. The optical fiber carries both the pump beam (green) and the signal (red). The light emitted by the dye molecules passes through the transparent walls and scatters within the external medium. The external particles are not in scale.

in-vivo applications. Finally, these techniques also have the drawback of altering the sample, so precluding applications such as quality check in industrial production lines.

To overcome these problems, we recently proposed and realized a new kind of random laser based sensor [4]. By maintaining a clear physical separation between the active material and the scattering sample, the sensor can do less invasive measurements with negligible disturbance of the material under study. An above threshold emission arises if the back scattered light from the external sensed medium is strong enough to make the stimulated emission prevail upon the spontaneous emission. Such a structure bypasses the invasive treatment for the investigated sample, that remains untouched by the sensing process. In that work [4] we showed that the output signal of the random laser sensor, and in particular the emission spectrum, thanks to the nonlinear behavior of a laser near threshold, is highly sensitive to the scattering characteristics of an external sample. By performing measurements with different concentrations of the same scattering material, we showed that intensity and wavelength shift of the spectrum peak are strongly connected to the scattering properties of the sample. In the present work, we report on the capability of technique based on such a sensor to quantify diffusive characteristics of a disordered sample. Thus, the goal of this work is to prove that the μ'_s of the external medium is the key parameter characterizing the sensor's emission, whatever external medium is used. The

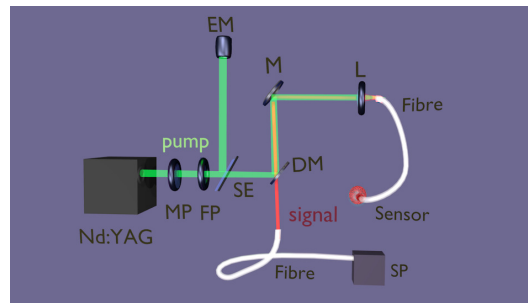


Fig. 3. Scheme of experimental set-up: MP movable polarizer, FP fixed polarizer, SE semi-transparent plate, EM energy meter, DM dichroic mirror, M mirror, L lens, SP spectrometer.

method appears suitable to a quantitative direct analysis by means of a simple comparison with a standard and inexpensive sample such as Intralipid20%, high characterized in literature.

In Sec. 2 a further insight about the method proposal is provided, focusing the main concepts and the experimental procedure idea. In Sec. 3 and in Sec. 4 the samples preparation, the sensor structure and the experimental setup are described. Finally, in the last two sections the experimental results are showed and discussed.

2. Method core

Before entering in the details of the experiment, here we describe our idea of a method for a direct measurement of μ'_s .

The main point of the method is the calibration of the set-up by using a well-known material such as Intralipid20%. Indeed, in the previous paper [4], we demonstrated the high sensitivity of the sensor on the variation of the scattering properties of an external scattering medium. In particular, we showed that, for a fixed value of pumping energy, one achieves an intensity of the signal dependent on the different dilution of Intralipid20%. In the present work, we show the promising results about the ability of the sensor to measure the μ'_s of samples composed by different concentrations of different scatterers.

Then, we present the results for different scattering media composed by calibrated samples, where the same value of μ'_s can be obtained by sets of spheres of different sizes. The starting hypothesis consisted in considering μ'_s as the main macroscopic parameter that quantifies the amount of radiation that, once spontaneously emitted by the sensor and after a random propagation inside the external medium, eventually reaches it again and undergoes amplification by stimulated emission.

Here we experimentally test this hypothesis and its limit of validity.

3. Sample preparation

Two different kinds of samples of scattering media have been prepared: a calibrated scattering material (dilution of Intralipid20% in water), whose characteristics are well described from the literature once its concentration is known, and samples composed by calibrated microspheres (a suspension of polystyrene latex spheres in water), whose concentration can be *a priori* calculated, with Mie theory, to obtain the same scattering properties.

In literature there are few scattering media with a high characterization of their scattering properties; among them, the inexpensive Intralipid20%, a fat emulsion in water, is of great importance for its high stability, reproducibility and absorption coefficient very close to the water

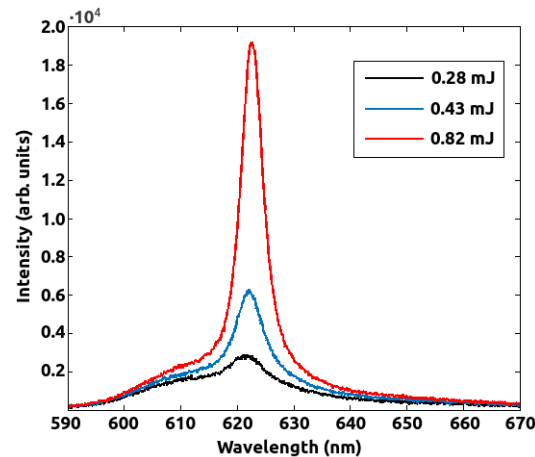


Fig. 4. Examples of signal spectra from a sample ($\mu'_s = 2.33 \text{ mm}^{-1}$) composed by a water dispersion of polystyrene particles of 190 nm diameter. The pump pulse has three different energies.

value [42,43]. Hence, it is widely used, as calibrated diffusive medium [44]. This medium is a water dilution of a fat emulsion of different components, consisting in a polydispersion of particles whose diameter spans from 50 to 700 nm. A water dilution of Intralipid20% was prepared in order to achieve a calibrated medium with a chosen μ'_s . The extensive characterization that can be found in literature allows to prepare a sample with a chosen μ'_s just preparing the correct dilution [12,43–48].

Regarding the samples containing calibrated spherical particles dispersion, the concentrations, needed to obtain the required scattering coefficient μ'_s , were derived from a calculation based on Mie theory (see Appendix). The original samples, all composed by uniform polystyrene latex microspheres (absolute refractive index of 1.589) suspended in water, were provided by Sigma-Aldrich and by Magsphere Inc. (table 3). For each sample, the manufacturers provided the mass fraction of the dispersion, the average value and the standard deviation of the particles diameters distribution. These values are in good agreement with what we can argue by an electron microscope image reported in Fig. 1. In table are also shown the values of the μ_s calculated by Mie theory for each sample. The different values of μ_s for the different samples are due to the single scattering properties of the particles of different sizes. Hence, once calculated the suitable water dilution for each original particle sample, one has different scattering media composed by particles of different diameter, with orders of magnitude that span from $\approx 100 \text{ nm}$ to $\approx 2 \mu\text{m}$, *a priori* characterized by the same μ'_s . Hence, from theoretical point of view, the samples as prepared, characterized by very different particle concentrations, have the same value of μ'_s . Moreover, the samples are subjected to ultrasonic bath in order to remove and prevent clustering and then altering the scattering properties of the turbid media.

In summary, the chosen μ'_s for the microspheres samples and for the Intralipid20%, dilution is $\mu'_s = 2.33 \text{ mm}^{-1}$, that corresponds to 0.430 mm of transport mean free path, a value typical of diffusive media such as biological tissues. For all samples the absorption coefficient can be neglected compared to the reduced scattering coefficient. The dimensions of the scattering cell (1 cm side) are wide enough to have a large number of photons scattered back to the sensor.

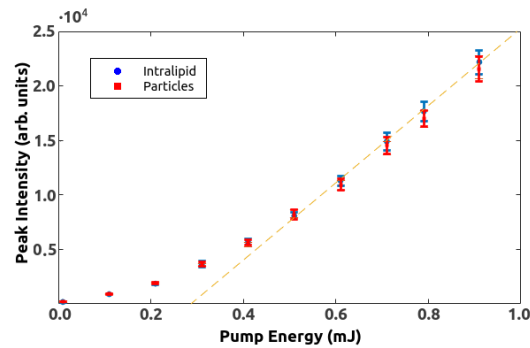


Fig. 5. Peak intensity of the signal spectrum for a dilution of Intralipid20% (blue) and a dispersion of particle of 190 nm diameter (red) (Sigma-Aldrich) as a function of pump energy. Both samples have $\mu'_s = 2.33 \text{ mm}^{-1}$. The dashed line is the linear fit of the five larger values for the signal of Intralipid20% and a threshold value around 0.3 mJ.

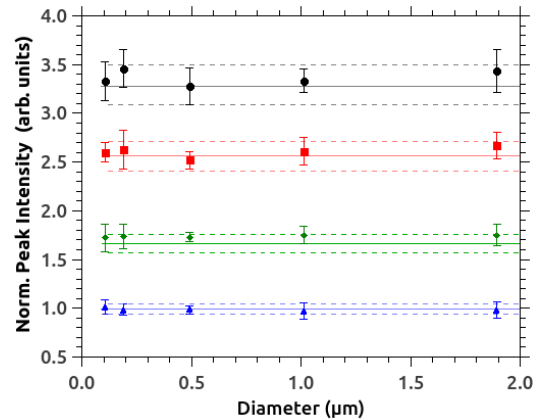


Fig. 6. Peak intensity of the signal spectrum (normalized to the water value) for different particle size (Sigma-Aldrich) at different pump energies: 0.19 mJ (blue triangles), 0.39 mJ (green rhombus), 0.65 mJ (red squares) and 0.89 mJ (black circles). The continuous and dashed lines respectively show the correspondent mean value and standard deviation of the measurement with Intralipid20% at the same μ'_s and pump energies. Within the precision of the measurement, the peak intensity is constant for a fixed pump energy. The Intralipid20% lines are reported down to the diameter of $\approx 100 \text{ nm}$, below which the microspheres signals are no longer consistent with the reference medium.

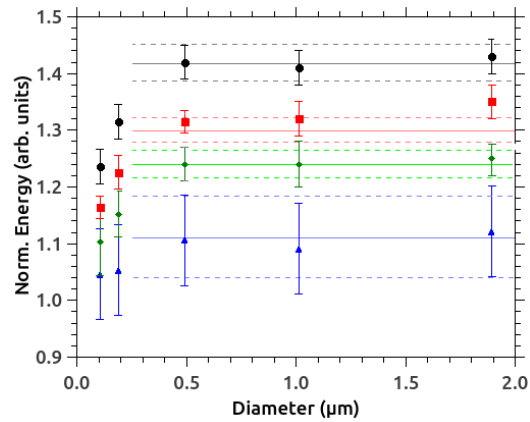


Fig. 7. The energy of the signal (normalized to the water value) for different particle size (Sigma-Aldrich) at different pump energies: 0.19 mJ (blue triangles), 0.39 mJ (green rhombus), 0.65 mJ (red squares) and 0.89 mJ (black circles). The continuous and dashed line respectively show the correspondent mean value and uncertain (80% of its standard deviation, for sake of clarity) of Intralipid20%, at the same the measurement with μ'_s and pump energies. The Intralipid20% lines are reported down to the diameter of ≈ 250 nm, below which the microspheres signals are no longer consistent with the reference medium.

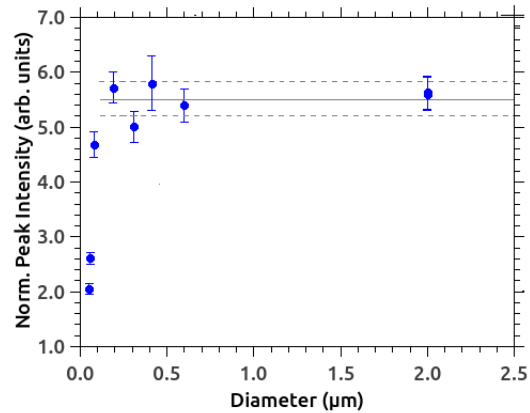


Fig. 8. Peak intensity of the signal (normalized to the water value) for different particle size (Magsphere Inc.) at the pump energy: 1.39 mJ. The continuous and dashed gray line respectively show the correspondent mean value and standard deviation of the measurement with Intralipid20% at the same μ'_s and pump energy. The Intralipid20% lines are reported down to the diameter of ≈ 100 nm, below which the microspheres signals are no longer consistent with the reference medium.

Table 1. Data of the samples with calibrated spheres. For all the samples, the particles concentration is set to achieve the same $\mu'_s = 2.33 \text{ mm}^{-1}$. The scattering coefficient μ_s is also reported.

Diameter (μm)	σ (μm)	μ_s (mm^{-1})	Manufacturer
0.050	0.011	2.38	Magsphere Inc.
0.058	0.009	2.39	Magsphere Inc.
0.080	0.011	2.45	Magsphere Inc.
0.107	0.003	2.56	Sigma-Aldrich
0.190	0.006	3.31	Sigma-Aldrich
0.19	0.03	3.34	Magsphere Inc.
0.31	0.03	7.05	Magsphere Inc.
0.41	0.02	9.58	Magsphere Inc.
0.493	0.012	13.2	Sigma-Aldrich
0.60	0.06	16.5	Magsphere Inc.
1.01	0.02	29.1	Sigma-Aldrich
1.89	0.04	28.4	Sigma-Aldrich
2.00	0.12	25.9	Magsphere Inc.

4. Experimental set-up

The random laser optical sensor is schematically shown in Fig. 2. The sensors used in that work are all homemade by glassblowing. It consists in a spherical glass cell open on top to allow the insertion of an optical fiber (core diameter of $900 \mu\text{m}$) carrying both the input pump beam and the output signal produced within the sensor. The spherical cell of diameter $\approx 3 \text{ mm}$ is filled by a suitable concentration of an alcoholic solution of an organic dye, as the gain medium, and a small quantity of dispersed ZnO nanoparticles, added in order to introduce a small loss factor to avoid the onset of laser amplification caused by reflections at the container walls. Once irradiated by a pump pulse, a population inversion is established among the dye molecules, that initially emit radiation by spontaneous emission. Such a radiation passes through the transparent wall of the sensor and propagates into the external scattering medium. After random paths inside the disordered sensed medium, an amount of light can go back to the sensor, crossing again the cell walls and thus undergoing amplification by stimulated emission in the active medium. Hence, the external disordered medium provides a feedback signal for the random laser emission, in a way that strongly depends on the characteristics of the single scatterers and on their concentration. The mechanism gives to the sensor its non-invasive properties, since no injection of gain material in the sensed sample and no direct irradiation are required.

In Fig. 3 a schematic diagram of the experimental set-up is shown. The pump beam is provided by a frequency-doubled Q-switched Nd:YAG at a repetition rate of 2 Hz. The pumping energy is tuned by a pair of polarizers: one (MP) can be rotated by a stepper motor controlled by a PC and the other is fixed (FP). A reflection from a semi-transparent plate (SE) is sent to an energy meter (EM) to detect the energy of each pump pulse. The pump beam is focalized by a

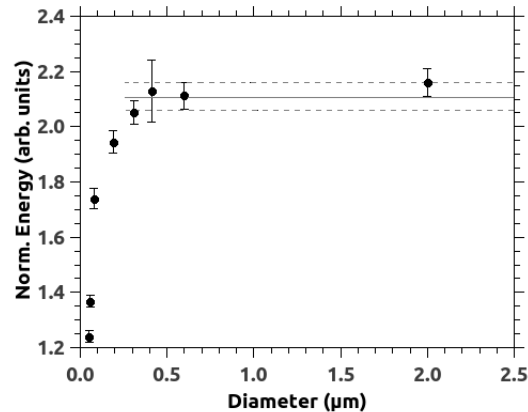


Fig. 9. The energy of the signal (normalized to the water value) for different particle size (Magsphere Inc.) at the pump energy: 1.39 mJ. The continuous and dashed gray line respectively show the correspondent mean value and standard deviation of the measurement with Intralipid20% at the same μ'_s and pump energy. The Intralipid20% lines are reported down to the diameter of ≈ 250 nm, below which the microspheres signals are no longer consistent with the reference medium.

lens (L) to the input of the sensor fiber, with a coupling efficiency of about 32%. The random laser signal coming back from the sensor is extracted by the dichroic mirror (DM) and injected into the input fiber of the spectrometer (SP). The spectrometer has a resolution of 0.25 nm. An automatic acquisition system allows to store the spectrum of each signal pulse and the energy of the corresponding pump pulse.

The diffusive samples are put in a square container with black walls with a side of 1.0 cm. The sensor is partially immersed inside the liquid sample at the same fixed depth (for the half of the sensor diameter). The sensor is positioned at the center of the cross section of the cubic cell.

5. Results

The spectral behavior of the signal of the random laser sensor is determined by the scattering properties of the external medium and the energy of the pump pulse. In Fig. 4 we report typical spectra for the random laser signal from a scattering sample for three different pump energies.

In Fig. 5 the peak intensity of the signal, as a function of the pump energy, is shown for a sample of particles with a mean diameter of 190 nm (Sigma-Aldrich) and a dilution of Intralipid20%, at the same μ'_s . It is worthwhile to stress that the two signals remain consistent upon the whole range of pump energies, indicating that the critical parameter for the process is μ'_s . Moreover, the linear fit of the five larger values for Intralipid20% allows to highlight the threshold behavior of the signal. Such a threshold can be estimated around 0.3 mJ. Indeed, unlike a laser, random lasing does not show a single threshold value, but an energy zone characterized by a changing of the slope of the trend of the peak intensity versus the pump energy.

To check this result, we sensed samples with the same μ'_s but with very different microsphere diameters. In Fig. 6 the peak intensity, normalized to the water value, is shown as a function of particle sizes at different pump energies (0.19 mJ, 0.39 mJ, 0.65 mJ and 0.89 mJ). The mean value of Intralipid20% signal is also reported for the corresponding energies as straight line, besides their uncertain as dashed lines. As a worth result, the peak intensity is independent of the diameter in the range analyzed (from ≈ 100 nm to ≈ 2 μm). Furthermore, the peak intensity

is consistent to that of Intralipid20% with the same μ'_s . These results indicate that, by previous calibration of the sensor with reference medium (Intralipid20%), the μ'_s of a material is directly measurable by a fast and simple procedure.

Figure 7 shows the total energy of the spectrum, i.e. its integral. The same behavior of the peak intensity is shown, with the exception of the two smallest particles, that exhibits lower values. Then, for the smallest particles the total energy of the signal shows a behavior dependent on the particle dimension. Such a deviation suggests a possible method to determine the dimension of the smaller particles by means of the comparison between the peak value and the energy of the spectrum.

To extend our measurement to spheres of smaller diameter down to ≈ 50 nm and check the robustness of the method, we repeated the experiment with a second sensor and with microspheres of a different manufacturer (Magsphere Inc.). The results for the peak intensity and the energy of the spectrum are reported in Figs. 8 and 9 respectively. These results are in good agreement with the previous ones. The peak is independent of the dimension down to ≈ 100 nm. Again, the μ'_s is the determining parameter for the intensity of the peak from ≈ 100 nm to $\approx 2\mu\text{m}$, while it shows a dependence on the diameter below such a range. The energy of the spectrum (Fig. 9) show a behavior dependent on particles dimension under ≈ 250 nm.

In summary, the obtained results show that it is possible to measure μ'_s of a scattering medium by a calibration of the random laser sensor. The results also show a dependence on the dimension of the scatterers that in future may be investigated to obtain information about particles size.

Although these results have been presented for one single value of μ'_s in the external medium, we argue that there are not physical reasons to have a different behavior for other values of μ'_s . In fact, as shown in [4], the sensor signal is sensitive to a wide range of concentration of scatterers of the external medium. However, a future measurement for different μ'_s can improve the characterization of the sensor response.

6. Conclusions

Our experimental results on the random laser sensor performance show that there is only one characteristic, i.e. the transport mean free path (the reciprocal of μ'_s) of the light within the medium, that determines the peak intensity of the spectrum in the medium, for the range of scatterers dimension between ≈ 100 nm and $\approx 2\mu\text{m}$. An easy calibration with a well characterized and inexpensive material indicates the possibility of a fast and direct measurement of μ'_s . Moreover, the results show that, for diameters below ≈ 250 nm, the peak intensity and the integral of the spectrum have a different behavior, suggesting a possible method to retrieve information about scatterers dimension of the sample under study. In addition, the method appears robust against a homemade realization of the sensor. In fact, the quality of the signal in terms of intensity and spectral characteristics has been reproducible for different realizations of the sensor.

The method here proposed can be also implemented for other dyes used in the sensor, so providing different probing wavelengths that could be more suitable for investigating other kinds of sample.

Appendix: Microspheres concentration calculation

The reduced scattering coefficient μ'_s , for a monodispersion of spherical particles, is given by [5]:

$$\mu'_s = \frac{3}{4}\rho_v \frac{Q(1-g)}{r} \quad (1)$$

where ρ_v is the fractional volume of the particles, r the particle radius, Q the scattering efficiency and g the asymmetry factor of the scattering function. Q and g describe the single particle light scattering behavior and are in general complicated functions of the relative refractive index of the scatterer n_r and the size parameter $x = 2\pi r/\lambda_b$, where λ_b is the radiation wavelength in the bulk

material. To obtain the desired scattering coefficient, the concentration of each sample, achieved by adding pure water, has been fixed according to equation 1, given the size of the particle and the refractive index of the material, once the single particle coefficients Q and g are calculated by a program based on Mie theory [49].

In order to increase the accuracy in determining the sample concentration, the deviation of Q and g upon the different wavelengths of the dye emission spectrum and upon the size distribution of the particles radius must be considered. For the sizes of scattering particles we assumed a lognormal distribution with the mean value \bar{r} provided by the suppliers.

$$f(r) = \frac{1}{rS\sqrt{2\pi}} \exp \left[-\frac{1}{2} \left(\frac{\ln r - m}{S} \right)^2 \right] \quad (2)$$

where:

$$m = \ln \left(\frac{\bar{r}^2}{\sqrt{\sigma^2 + \bar{r}^2}} \right) \quad (3)$$

$$S = \sqrt{\ln \left(\frac{\sigma^2}{\bar{r}^2} + 1 \right)} \quad (4)$$

Fixed the wavelength, the scatterer parameters Q and g are obtained by averaging over the sphere radius distribution:

$$Q(\lambda) = \int_0^\infty dr f(r) Q(r, \lambda) \quad (5)$$

$$g(\lambda) = \int_0^\infty dr f(r) g(r, \lambda) \quad (6)$$

Acknowledgments

Acknowledgements are due to Andrea Barucci, Franco Cosi, Daniele Farnesi, Simone Berneschi and Gualtiero Nunzi Conti (IFAC-CNR) for contributions to fabricating the sensor, to Danilo Marcucci for fabricating the sample container and to Stefano Caporali for providing the particles images at the electron microscope.

References

1. T. Durduran, R. Choe, W. B. Baker, and A. G. Yodh, "Diffuse optics for tissue monitoring and tomography," *Rep. Prog. Phys.* **73**, 076701 (2010).
2. D. R. Leff, O. J. Warren, L. C. Enfield, A. Gibson, T. Athanasiou, D. K. Patten, J. Hebden, G. Z. Yang, and A. Darzi, "Diffuse optical imaging of the healthy and diseased breast: A systematic review," *Breast Cancer Res. Treat.* **108**(1), 9–22 (2008).
3. S. L. Jacques, "Optical properties of biological tissues: a review," *Phys. Med. Biol.* **58**(11), R37 (2013).
4. E. Ignesti, F. Tommasi, L. Fini, F. Martelli, N. Azzali, and S. Cavalieri, "A new class of optical sensors: a random laser based device," *Sci. Rep.* **6**, 35225 (2016).
5. F. Martelli, S. Del Bianco, A. Ismaelli, and G. Zaccanti, *Light Propagation through Biological Tissue and other Diffusive Media* (SPIE Press/Bellingham, Whashington (USA), 2009).
6. B. Chance, ed., *Photon Migration in Tissues* (Plenum Press, 1989).
7. A. Taddeucci, F. Martelli, M. Barilli, M. Ferrari, and G. Zaccanti, "Optical properties of brain tissue," *J. Biomed. Opt.* **1**(1), 117–123 (1996).
8. F. Martelli, S. Del Bianco, L. Spinelli, S. Cavalieri, P. Di Ninni, T. Binzoni, A. Jelzow, R. Macdonald, and H. Waibnitz, "Optimal estimation reconstruction of the optical properties of a two-layered tissue phantom from time-resolved single-distance measurements," *J. Biomed. Opt.* **20**, 115001 (2015).
9. M. Patterson, B. Chance, and B. Wilson, "Time resolved reflectance and transmittance for the non-invasive determination of tissue optical properties," *Appl. Opt.* **28**, 2231–2336 (1989).
10. H. van Staveren, C. Moes, J. van Marle, S. Prahl, and M. van Gemert, "Light scattering in intralipid-10% in the wavelength eange of 400-1100 nm," *Appl. Opt.* **30**, 4507–4514 (1991).
11. L. Spinelli, F. Martelli, A. Farina, A. Pifferi, A. Torricelli, R. Cubeddu, and G. Zaccanti, "Calibration of scattering and absorption properties of a liquid diffusive medium at nir wavelengths. time-resolved method," *Opt. Express* **15**(11), 6589–6604 (2007).

12. L. Spinelli, M. Botwicz, N. Zolek, M. Kacprzak, D. Milej, P. Sawosz, A. Liebert, U. Weigel, T. Durduran, F. Foschum, A. Kienle, F. Baribeau, S. Leclair, J.-P. Bouchard, I. Noiseux, P. Gallant, O. Mermut, A. Farina, A. Pifferi, A. Torricelli, R. Cubeddu, H.-C. Ho, M. Mazurenka, H. Wabnitz, K. Klauenberg, O. Bodnar, C. Elster, M. Bénazech-Lavoué, Y. Bérubé-Lauzière, F. Lesage, D. Khoptyar, A. A. Subash, S. Andersson-Engels, P. Di Ninni, F. Martelli, and G. Zaccanti, "Determination of reference values for optical properties of liquid phantoms based on intralipid and india ink," *Biomed. Opt. Express* **5**(7), 2037–2053 (2014).
13. S. J. Madsen, E. R. Anderson, R. C. Haskell, and B. J. Tromberg, "Portable, high-bandwidth frequency-domain photon migration instrument for tissue spectroscopy," *Opt. Lett.* **19**(23), 1934–1936 (1994).
14. S. Fantini, M. A. Franceschini, J. B. Fishkin, B. Barbieri, and E. Gratton, "Quantitative determination of the absorption spectra of chromophores in strongly scattering media: a light-emitting-diode based technique," *Appl. Opt.* **33**(22), 5204–5213 (1994).
15. S. Fantini, M. Franceschini-Fantini, J. Maier, S. Walker, B. Barbieri, and E. Gratton, "Frequency domain multichannel optical detector for non-invasive tissue spectroscopy and oximetry," *Opt. Eng.* **34**(1), 32–42 (1995).
16. L. Bressel, R. Hass, and O. Reich, "Particle sizing in highly turbid dispersions by photon density wave spectroscopy," *J. Quant. Spectrosc. Radiat. Transf.* **126**, 122–129 (2013).
17. M. Humar and S. H. Yun, "Intracellular microlasers," *Nat. Photonics* **9**, 572–576 (2015).
18. M. Schubert, A. Steude, P. Liehm, N. M. Kronenberg, M. Karl, E. C. Campbell, S. J. Powis, and M. Gather, "Lasing within live cells containing intracellular optical microresonators for barcode-type cell tagging and tracking," *Nano Lett.* **15**, 5647–5652 (2015).
19. V. S. Letokhov, "Generation of light by scattering medium with negative resonance absorption," *Eksp. Teor. Fiz.* **53**, 1442 (1967).
20. D. S. Wiersma, "The physics and applications of random lasers," *Nat. Phys.* **4**, 359 (2008).
21. H. Cao, "Random lasers: Development, features and applications," *Opt. Photonics News* **16**, 24–29 (2005).
22. S. H. Choi and Y. L. Kim, "The potential of naturally occurring lasing for biological and chemical sensors," *Biomed. Eng. Lett.* **4**(3), 201–212 (2014).
23. M. Gaio, S. Caixeiro, B. Marelli, F. G. Omenetto, and R. Sapienza, "Gain-based mechanism for pH sensing based on random lasing," *Phys. Rev. Appl.* **7**, 034005 (2017).
24. Y. Xu, L. Zhang, S. Gao, P. Lu, S. Mihailov, and X. Bao, "Highly sensitive fiber random-grating-based random laser sensor for ultrasound detection," *Opt. Lett.* **42**(7), 1353–1356 (2017).
25. M. Noginov, H. Caulfield, N. Noginova, and P. Venkateswarlu, "Line narrowing in the dye solution with scattering centers," *Opt. Commun.* **118**, 430 (1995).
26. H. Cao, Y. G. Zhao, S. T. Ho, E. W. Seelig, Q. H. Wang, and R. P. H. Chang, "Random laser action in semiconductor powder," *Phys. Rev. Lett.* **82**, 2278–2281 (1999).
27. H. Cao, J. Y. Xu, D. Z. Zhang, S.-H. Chang, S. T. Ho, E. W. Seelig, X. Liu, and R. P. H. Chang, "Spatial confinement of laser light in active random media," *Phys. Rev. Lett.* **84**, 5584–5587 (2000).
28. N. M. Lawandy, R. M. Balachandran, A. S. L. Gomes, and E. Suvain, "Laser action in strongly scattering media," *Nature* **368**, 436 (1995).
29. D. S. Wiersma and A. Lagendijk, "Light diffusion with gain and random lasers," *Phys. Rev. E* **54**, 4256 (1996).
30. R. Uppu, A. K. Tiwari, and S. Mujumdar, "Identification of statistical regimes and crossovers in coherent random laser emission," *Opt. Lett.* **37**(4), 662 (2012).
31. E. Ignesti, F. Tommasi, L. Fini, S. Lepri, V. Radhalakshmi, D. S. Wiersma, and S. Cavalieri, "Experimental and theoretical investigation of statistical regimes in random laser emission," *Phys. Rev. A* **88**, 033820 (2013).
32. F. Tommasi, E. Ignesti, L. Fini, and S. Cavalieri, "Controlling directionality and the statistical regime of the random laser emission," *Phys. Rev. A* **91**, 033820 (2015).
33. M. Siddique, L. Yang, Q. Wang, and R. Alfano, "Mirrorless laser action from optically pumped dye-treated animal tissues," *Opt. Commun.* **117**(5), 475 – 479 (1995).
34. M. Wang, D. Liu, N. He, and S. L. Jacques, "Biological laser action," *Appl. Opt.* **35**(10), 1775 – 1779 (1996).
35. R. C. Polson and Z. V. Vardeny, "Organic random lasers in the weak-scattering regime," *Phys. Rev. B* **71**, 045205 (2005).
36. Q. Song, S. Xiao, Z. Xu, J. Liu, X. Sun, V. Drachev, V. M. Shalaev, O. Akkus, and Y. L. Kim, "Random lasing in bone tissue," *Opt. Lett.* **35**(9), 1425–1427 (2010).
37. D. Zhang, G. Kostovski, C. Karnutsch, and A. Mitchell, "Random lasing from dye doped polymer within biological source scatters: The pomponia imperialiorum cicada wing random nanostructures," *Org. Electron.* **13**(11), 2342 – 2345 (2012).
38. C.-S. Wang, T. Chang, T.-Y. Lin, and Y.-F. Chen, "Biologically inspired flexible quasi-single-mode random laser: An integration of peris canidia butterfly wing and semiconductors," *Sci. Rep.* **4**, 6736 (2014).
39. R. C. Polson and Z. V. Vardeny, "Random lasing in human tissues," *Appl. Phys. Lett.* **85**, 1289 (2004).
40. Y. Wang, Z. Duan, Z. Qiu, P. Zhang, J. Wu, D. Zhang, and T. Xiang, "A new class of optical sensors: a random laser based devicerandom lasing in human tissues embedded with organic dyes for cancer diagnosis," *Sci. Rep.* **7**, 8385 (2017).
41. F. Lahoz, I. R. Martín, M. Urgellís, J. Marrero-Alonso, R. Marín, C. J. Saavedra, A. Boto, and M. Diaz, "Random laser in biological tissues impregnated with a fluorescent anticancer drug," *Laser Phys. Lett.* **12**, 045805 (2015).
42. H. J. van Staveren, C. J. M. Moes, J. van Marie, S. A. Prahl, and M. J. C. van Gemert, "Light scattering in

- Intralipid-10% in the wavelength range of 400–1100 nm,” *Appl. Opt.* **30**(31), 4507–4514 (1991).
43. R. Michels, F. Foschum, and A. Kienle, “Optical properties of fat emulsions,” *Opt. Express* **16**, 5907–5925 (2008).
 44. P. Di Ninni, F. Martelli, and G. Zaccanti, “Intralipid: towards a diffusive reference standard for optical tissue phantoms,” *Phys. Med. Biol.* **56**(2), N21 (2011).
 45. F. Martelli and G. Zaccanti, “Calibration of scattering and absorption properties of a liquid diffusive medium at near wavelengths. cw method,” *Opt. Express* **15**(2), 486–500 (2007).
 46. G. Zaccanti, S. Del Bianco, and F. Martelli, “Measurements of optical properties of high-density media,” *Appl. Opt.* **42**, 4023–4030 (2003).
 47. P. Di Ninni, Y. Bérubé-Lauzière, L. Mercatelli, E. Sani, and F. Martelli, “Fat emulsions as diffusive reference standards for tissue simulating phantoms?” *Appl. Opt.* **51**(30), 7176–7182 (2012).
 48. B. Aernouts, E. Zamora-Rojas, R. V. Beers, R. Watté, L. Wang, M. Tsuta, J. Lammertyn, and W. Saeys, “Supercontinuum laser based optical characterization of intralipid phantoms in the 500-2250 nm range,” *Opt. Express* **21**(26), 32450–32467 (2013).
 49. C. F. Bohren and D. Huffman, *Absorption and scattering of light by small particles*, Wiley science paperback series (Wiley, 1983).